

RENDICONTI LINCEI MATEMATICA E APPLICAZIONI

GIACINTO PORCO, GIUSEPPE SPANDEA, RAFFAELE
ZINNO

On the nonlinear behaviour of bimodular multilayer ed plates.

*Atti della Accademia Nazionale dei Lincei. Classe di Scienze Fisiche,
Matematiche e Naturali. Rendiconti Lincei. Matematica e Applicazioni,
Serie 9, Vol. 2 (1991), n.4, p. 317–337.*

Accademia Nazionale dei Lincei

[<http://www.bdim.eu/item?id=RLIN_1991_9_2_4_317_0>](http://www.bdim.eu/item?id=RLIN_1991_9_2_4_317_0)

L'utilizzo e la stampa di questo documento digitale è consentito liberamente per motivi di ricerca e studio. Non è consentito l'utilizzo dello stesso per motivi commerciali. Tutte le copie di questo documento devono riportare questo avvertimento.

Atti della Accademia Nazionale dei Lincei. Classe di Scienze Fisiche, Matematiche e Naturali. Rendiconti Lincei. Matematica e Applicazioni, Accademia Nazionale dei Lincei, 1991.

Meccanica. — *On the nonlinear behaviour of bimodular multilayered plates.* Nota di GIACINTO PORCO, GIUSEPPE SPADEA e RAFFAELE ZINNO, presentata (*) dal Socio E. GIANGRECO.

ABSTRACT. — In an earlier study [16] the nonlinear behaviour of *unimodular* laminated plates was studied. This paper, following the previous study, concerns a large deflection analysis of moderately thick rectangular plates having arbitrary boundary conditions and finite thickness shear moduli. The plates are manufactured in *bimodular* materials and constructed in a *cross-ply* fashion or in a single layer with arbitrary fibre direction angle. Numerical results are obtained by a finite element technique in which are specified five degrees of freedom, three displacements and two bending slopes per node. Furthermore, the effects of plate aspect ratio, bimodularity ratio and fibre orientation are studied; finally, comparisons with some results available in literature are also given.

KEY WORDS: Plates; Bimodulus; Composites.

RIASSUNTO. — *Sul comportamento non lineare di piastre bimodulari multistrato.* In una precedente Nota [16] è stato studiato il comportamento non lineare di piastre laminate composite realizzate in materiale *unimodulare*. In questo lavoro, proseguendo lo studio precedente, viene analizzato il comportamento non lineare di piastre rettangolari moderatamente spesse arbitrariamente vincolate. Le piastre sono realizzate in materiale *bimodulare* e modellate secondo lo schema *cross-ply* ovvero in una singola lamina avente una arbitraria orientazione della direzione delle fibre. I risultati sono ottenuti adottando una tecnica computazionale agli elementi finiti considerando, per ogni nodo, cinque gradi di libertà: tre componenti di spostamento e due rotazioni flessionali. Inoltre vengono studiati gli effetti del rapporto di forma, del rapporto di bimodularità e della direzione delle fibre; vengono, infine, riportati alcuni confronti con risultati reperibili in letteratura.

NOTATION

A_{ij}, B_{ij}, D_{ij}	Exstensional, flexural-extensional and flexural stiffness ($i, j = 1, 2, 3$).
H_{ij}	Thickness shear stiffness ($i, j = 4, 5$).
a, b	Plate dimensions along the X and Y directions, respectively.
l	Index of the deformation's sign ($l = 1$ compression; $l = 2$ tension).
E_{1l}, E_{2l}	Layer elastic moduli in directions along fibres and normal to them.
$G_{12l}, G_{13l}, G_{23l}$	Layer in-plane and thickness shear moduli.
Ω	Midplane of the plate.
h	Total thickness of the laminate.
t_k	Thickness of k -th layer.
K	Shear correction coefficient.
x, y, z	Position coordinates in a cartesian system.
M_i, N_i	Stress couples and stress resultants, respectively ($i = x, y, xy$).
Q_i	Shear stress resultants ($i = x, y$).
u, v, w	Displacements in the x, y, z directions, respectively.
u_0, v_0, w_0	Displacements of the midplane in the x, y, z directions, respectively.
θ^k	Orientation of the k -th layer.
ψ_x, ψ_y	Slopes in the xz and yz planes.
$\chi_x, \chi_y, \chi_{xy}$	Curvature components.

(*) Nella seduta dell'11 maggio 1991.

$\varepsilon_x, \varepsilon_y, \varepsilon_{xy}$	Strain components.
$\varepsilon_x^0, \varepsilon_y^0, \varepsilon_{xy}^0$	Strain components in the middle surface.
n	Number of layers.
q_0	Uniform transverse load.
ν_{ij}	Poisson's ratios ($i, j = 1, 2 (i \neq j)$).
\bar{C}_{ij}^k	Material stiffness coefficient (local system) of the k -th layer.
C_{ij}^k	Material stiffness coefficient (global system) of the k -th layer.
$\varepsilon_1 = \varepsilon_f$	Strain in fibre direction.
z_{nx}, z_{ny}	Neutral surface position associated with $\varepsilon_x = 0$ and $\varepsilon_y = 0$, respectively.
z_{nn}	Neutral surface position associated with $\varepsilon_f = \varepsilon_1 = 0$.
K	Stiffness matrix of the plate.
F	Nodal force vector.
U	Nodal generalized displacement vector.

1. INTRODUCTION

Both at this time of rapid technological evolution and in the foreseeable future, applications in aeronautic, civil and mechanical fields, industrial production, and even in such areas as sports equipment, continuously require materials with an ever-growing range of properties.

The use of composite materials in structural applications is dictated by the outstanding strength, stiffness and low specific gravity of fibres, low maintenance costs, and strength in the preliminary design stage of complex vehicle structures. Composite materials in advanced underwater or space vehicles can result in significant increase in payload, weight reduction, range and speed, maneuverability, fuel efficiency and safety.

This increasing use of composite materials in structures has led to the requirement of more realistic mathematical modelling of the materials' behaviour and incorporation of this modeling in structural analyses [1].

Moreover, some composite materials exhibit a phenomenon known as *bimodularity* in which the elastic properties in tension differ from those in compression.

The analysis of these materials dates back to Saint Venant (1864) [2], continues in 1941 with Timoshenko [3] who considered the flexural stresses while Ambartsumyan [4] in 1965 introduced the terminology *bimodulus* and extended the concept to two-dimensional analysis.

The analysis of structures fabricated from these materials is usually more difficult than that of *conventional* composites, *i.e.* composites fabricated from laminae possessing equal values of tensile and compressive moduli, since it is not known *a priori* which parts of the structure are in tension and which are in compression. The resulting governing equations of bimodular structural elements in bending are dependent upon the unknown position of the neutral surface; therefore the analysis must be accomplished iteratively rather than directly.

Experimental evidence has shown that unidirectional glass fibres in an epoxy matrix have compression moduli about 0.8 times the tension moduli, while other unidirectional laminae (boron/epoxy) exhibit compression moduli higher (1.2 times circa)

than the tension moduli. Likewise some graphite/epoxy laminae have tension moduli higher than compression moduli (up to 40%) whereas carbon/carbon laminae can exhibit tension moduli from two to five times greater than the compression moduli [5].

This pattern shows the extreme variability in the material properties of fibre reinforced laminates. Generally only micromechanics can furnish rational grounds for this circumstance. It is possible, however, to study the mechanical behaviour of composites manufactured with bimodular laminae by modeling their overall behaviour.

A macroscopic material model appropriate for bimodulus fibre-reinforced composites, usually named *fibre-governed* model, was proposed by Bert and subsequently found to agree well with experimental results [6].

In this model, the values of the elastic constants depend exclusively on the sign of the deformations in the fibre direction, and the different behaviour in tension and in compression is usually modeled using a bilinear stress-strain relationship with moduli E_t and E_c , which satisfactorily approximate the actual nonlinear behaviour of materials.

Strictly speaking all these materials behave more or less nonlinearly, even in the very small strain state. However, since the nonlinearity for small strains is of a minor nature, and in view of the difficulty of analysing problems involving nonlinear materials, the stress-strain relation of such materials is often approximated by two straight lines, with slope discontinuity at the origin. In other words, the material behaviour is specified approximately in two different elastic constants, whose selection is governed by whether the stress state is one of tension or compression. Models of linearised bimodulus materials concern both isotropic [7] and anisotropic laminae [8, 9] and multilayered plates [10].

The previous analyses of composite laminated plates made of bimodulus materials are almost all limited to thin plates and only to cases of geometrical linearity. But a comparison of results obtained from the classical plate theory (Kirchhoff-Love theory) with the effective deflection of layered composite plates indicates the necessity of considering transverse shear deformation (Mindlin's plate model).

In fact transverse shear effects are more important in composite laminated plates than in isotropic ones because of their low transverse shear moduli relative to the in-plane Young's moduli. The analysis of composite moderately thick plates requires the consideration of the effects of transverse shear deformation, generally named as FSDT (First order Shear Deformation plate Theory) [11], and of nonlinear terms in the strain-displacement relationship in the sense of von Karman [12, 13].

To the best knowledge of the authors, the effect of the fibre direction angle on the nonlinear behaviour of bimodular Mindlin's plates has, to date, yet to be analysed satisfactorily.

Gordaninejad [14, 15] in two papers published in 1989 analyses the nonlinear behaviour of thin bimodular plates and the linear behaviour of thick bimodular plates.

In this work the analysis of thick bimodular plates takes into account the nonlinear

terms in the strain-displacement relationships in the sense of von Karman, and the effect of shear deformation is included by considering the First order Shear Deformation plate Theory.

2. ANALYSIS

Let Ω be a simply connected region of \mathbf{R}^2 with its regular boundary $\partial\Omega$; a plate P of thickness b in the undeformed state is defined by the cartesian product of points in the midplane Ω and the normal $[-b/2, +b/2]$

$$P = \Omega \times [-b/2; +b/2].$$

Let $(0, x, y, z)$ be a cartesian coordinate system with origin at 0 and with x, y axes complanar to Ω and oriented as indicated in figs. 1a, 1b; the local coordinate system is shown in fig. 2.

In this work plates consisting of n layers oriented at 0° and 90° to the plate axes (fig. 1a), defined as a *cross-ply* plates, are studied; furthermore rectangular fibrous composite plates with constant thickness b and fibres oriented at an arbitrary angle θ (fig. 1b) are also considered.

As discussed earlier each lamina has different orthotropic moduli in tension (E_t) and compression (E_c) with nonlinear behaviour modeled by a bilinear stress-strain relation (fig. 3).

Many results relative to the behaviour of laminates made of materials with the same moduli in tension and compression are known [16].

In unimodular symmetric laminates, there is no coupling between bending and extension, while in unsymmetric laminates the effect of coupling dies out very rapidly as the number of layers increases. Similar conclusions cannot be drawn for laminates fabricated in materials with different moduli in tension and in compression. Thus a laminate which is apparently symmetric in geometry and in material properties with respect to its middle surface, is not symmetric when a load is applied and coupling between bending and stretching occurs.

Here, the analysis is developed by Mindlin's plate model, or «first order model», which takes into account the average shear deformability. Transverse shear effects are pronounced in composite laminated plates because of their low transverse shear moduli relative to the in-plane Young's moduli. Transverse shear strains can also be of significance in the analysis of isotropic plates with side-to-thickness ratios smaller than 20.

In the Mindlin-Reissner plate theory it is assumed that:

i) plane sections originally perpendicular to the middle plane of the plate remain plane, but not necessarily perpendicular to it;

ii) the axial deformation of segments parallel to z axis is zero.

Furthermore the normal stress in direction z is negligible when compared to the

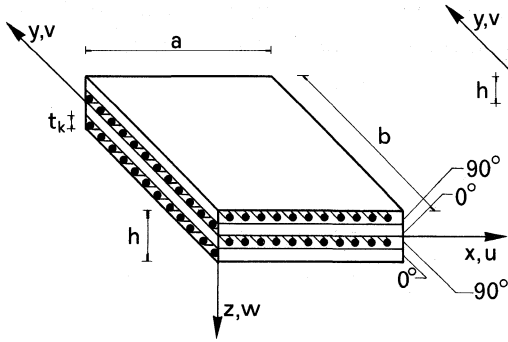


Fig. 1a. - Scheme of cross-ply laminate.

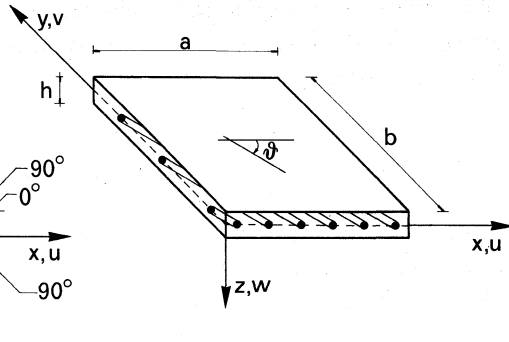


Fig. 1b. - Scheme of single-layer laminate.

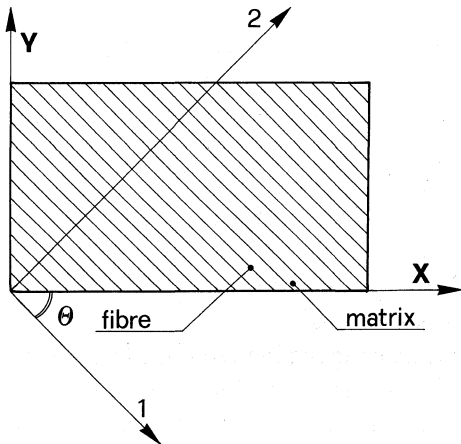


Fig. 2. - Global and natural directions.

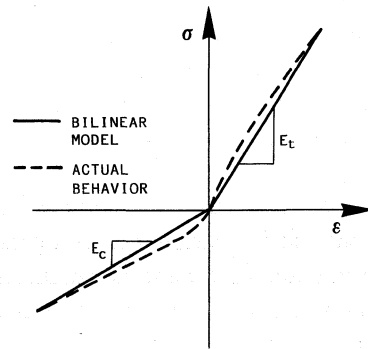


Fig. 3. - Bilinear stress-strain relation.

remaining stresses. Then, the displacement field is given by:

$$(1) \quad \begin{cases} u(x, y, z) = u_0(x, y) + z\psi_x(x, y); \\ v(x, y, z) = v_0(x, y) + z\psi_y(x, y); \\ w(x, y, z) = w_0(x, y); \end{cases}$$

where:

u, v and w , are, respectively, the displacements in the x, y, z directions; u_0, v_0 and w_0 are the corresponding midplane displacements, ψ_x and ψ_y are the bending slopes in the (xz) and (yz) planes.

Assuming that the transverse deflection is comparable to the total thickness of the plate, and that strains are much smaller than rotation, the nonlinear strain-displace-

ment relations can be taken as:

$$(2) \quad \begin{cases} \varepsilon_{xx} = u_{0,x} + w_{0,x}^2/2 + z\psi_{x,x} = \varepsilon_x^0 + z\chi_x; \\ \varepsilon_{yy} = v_{0,y} + w_{0,y}^2/2 + z\psi_{y,y} = \varepsilon_y^0 + z\chi_y; \\ \varepsilon_{zz} = (\psi_x^2 + \psi_y^2)/2; \\ 2\varepsilon_{xz} = \psi_x + w_{,x} = \gamma_{xz}; \\ 2\varepsilon_{yz} = \psi_y + w_{,y} = \gamma_{yz}; \\ 2\varepsilon_{xy} = u_{0,y} + v_{0,x} + w_{0,x}w_{0,y} + z(\psi_{x,y} + \psi_{y,x}) = \varepsilon_{xy}^0 + z\chi_{xy}. \end{cases}$$

In the general case of a plate consisting of n layers arbitrarily oriented and with reference to fig. 2, the constitutive equations of the k -th layer are expressed by eq. (3). Here $\bar{\sigma}_{ij}^k$ and $\bar{\varepsilon}_{ij}^k$ are the components of stress and strain tensors, respectively defined in the material coordinates $(1, 2, z)$, and \bar{C}_{ijl}^k are the material stiffness coefficients. In this relation the subscript l refers to compression ($l = 1$) or tension ($l = 2$) regions.

$$(3) \quad \begin{Bmatrix} \bar{\sigma}_{11l}^k \\ \bar{\sigma}_{22l}^k \\ \bar{\sigma}_{12l}^k \\ \bar{\sigma}_{13l}^k \\ \bar{\sigma}_{23l}^k \end{Bmatrix} = \begin{bmatrix} \bar{C}_{11l}^k & \bar{C}_{12l}^k & 0 & 0 & 0 \\ \bar{C}_{21l}^k & \bar{C}_{22l}^k & 0 & 0 & 0 \\ 0 & 0 & \bar{C}_{33l}^k & 0 & 0 \\ 0 & 0 & 0 & \bar{C}_{44l}^k & 0 \\ 0 & 0 & 0 & 0 & \bar{C}_{55l}^k \end{bmatrix} \begin{Bmatrix} \bar{\varepsilon}_{11l}^k \\ \bar{\varepsilon}_{22l}^k \\ \bar{\varepsilon}_{12l}^k \\ \bar{\varepsilon}_{13l}^k \\ \bar{\varepsilon}_{23l}^k \end{Bmatrix}.$$

Since among existing theories for modeling bimodular materials the fibre-governed compliance model has been shown to give better agreement with experimental results [6], this theory is adopted here to define the plane-stress reduced stiffnesses of the plate as follows:

$$(4) \quad \bar{C}_{ijl}^k = \bar{C}_{ijl}^k, \quad \text{if } \varepsilon_f < 0; \quad \bar{C}_{ijl}^k = \bar{C}_{ij2}^k, \quad \text{if } \varepsilon_f \geq 0.$$

Coefficients $\bar{C}_{ijl}^k = \bar{C}_{jil}^k$ are given (in terms of engineering constants) by:

$$(5) \quad \begin{cases} \bar{C}_{11l}^k = E_{1l}^k / (1 - \nu_{12l}^k \nu_{21l}^k); & \bar{C}_{12l}^k = \nu_{12l}^k E_{2l}^k / (1 - \nu_{12l}^k \nu_{21l}^k); \\ \bar{C}_{21l}^k = \nu_{21l}^k E_{1l}^k / (1 - \nu_{12l}^k \nu_{21l}^k); & \bar{C}_{22l}^k = E_{2l}^k / (1 - \nu_{12l}^k \nu_{21l}^k); \\ \bar{C}_{33l}^k = G_{12l}^k; & \bar{C}_{44l}^k = G_{13l}^k; & \bar{C}_{55l}^k = G_{23l}^k; \end{cases}$$

where:

$G_{12l}^k, G_{13l}^k, G_{23l}^k$, are the layer in-plane and thickness shear moduli;

E_{1l}^k, E_{2l}^k are the layer elastic moduli in directions along fibres (direction 1) and normal to them (direction 2);

ν_{12l}^k is the major Poisson's ratio;

$\nu_{21l}^k = (E_{2l}^k / E_{1l}^k) \nu_{12l}^k$ is the Poisson's ratio in direction 2 - 1.

Therefore for a unimodular orthotropic elastic medium (same moduli in tension and compression) as a consequence of the conditions of symmetry, and in the case of constitutive relations based on the plane-stress assumption, there are only

Furthermore Γ_i ($i = 1, \dots, 5$) are the portions (possibly overlapping) of the boundary $\partial\Omega$ of the midplane Ω on which \bar{N}_n , \bar{N}_s , \bar{M}_n , \bar{M}_s , \bar{Q}_n , respectively, are specified.

Moreover:

$$(8a) \quad (N_i, M_i) = \int_{-b/2}^{b/2} (1, z) \sigma_i dz \quad (i = x, y, xy),$$

$$(8b) \quad (Q_x, Q_y) = \int_{-b/2}^{b/2} (\tau_{zx}, \tau_{zy}) dz.$$

From eq. (3) transformed into global coordinates by eqs. (6) and (8a, b), we obtain the plate constitutive equations:

$$(9a) \quad \begin{Bmatrix} N_i \\ M_i \end{Bmatrix} = \begin{bmatrix} A_{ij} & B_{ij} \\ B_{ij} & D_{ij} \end{bmatrix} \begin{Bmatrix} \epsilon_j^0 \\ \chi_j \end{Bmatrix},$$

$$(9b) \quad \begin{Bmatrix} Q_x \\ Q_y \end{Bmatrix} = \begin{bmatrix} H_{44} & H_{45} \\ H_{54} & H_{55} \end{bmatrix} \begin{Bmatrix} \gamma_{xz} \\ \gamma_{yz} \end{Bmatrix}.$$

Here A_{ij} , B_{ij} , D_{ij} ($i, j = 1, 2, 3$) and H_{ij} ($i, j = 4, 5$) are the extensional, flexural-extensional and thickness shear stiffnesses respectively:

$$(10a, b) \quad A_{ij} = \sum_{k=1}^n \int_{b_{k-1}}^{b_k} C_{ij}^k dz, \quad B_{ij} = \sum_{k=1}^n \int_{b_{k-1}}^{b_k} C_{ij}^k z dz,$$

$$(10c, d) \quad D_{ij} = \sum_{k=1}^n \int_{b_{k-1}}^{b_k} C_{ij}^k z^2 dz, \quad H_{ij} = K^2 \sum_{k=1}^n \int_{b_{k-1}}^{b_k} C_{ij}^k dz,$$

and K^2 is the square of the shear correction coefficient [11].

The symbols b_k and b_{k-1} denote, respectively, the distances from the midplane of the plate to the lower and upper surface of the K -th layer.

In laminates containing bimodulus materials the evaluation of the plate stiffnesses (eqs. 10) is more complicated than in ordinary material laminates, because the individual layer plane-stress reduced stiffness can assume either one of two different values depending upon the appropriate neutral-surface locations.

Now, it is necessary to divide the general problem into two cases: cross-ply laminates (case *a*) and single layer laminates (case *b*).

CASE a).

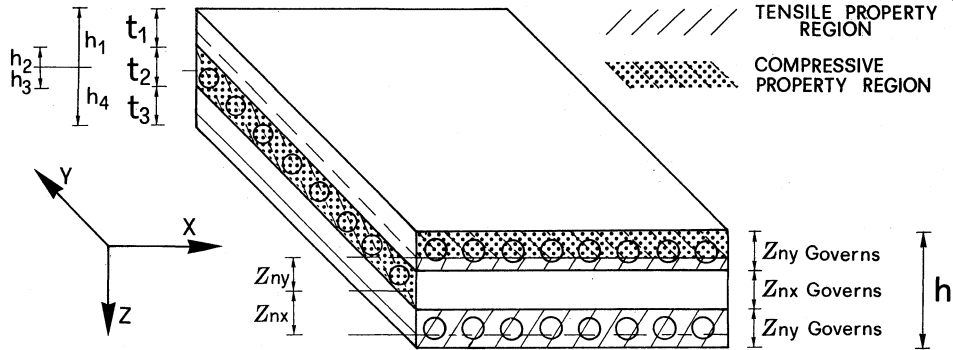


Fig. 4. - Scheme of a cross-ply laminate and position of neutral surfaces.

The elements of matrices (10) can be written as the neutral surface position becomes known, by determining z_{nx} and z_{ny} i.e. loci of points where $\epsilon_x = 0$ and $\epsilon_y = 0$ respectively.

Thus, from eqs. (2) we obtain:

$$(11a, b) \quad z_{nx} = -[u_{,x} + 1/2(w_{,x})^2] / \psi_{x,x}; \quad z_{ny} = -[v_{,y} + 1/2(w_{,y})^2] / \psi_{y,y}.$$

From these values, by means of the procedure that will be described in the next section, it is possible to determine the matrices **A, B, D** and **H**.

For example, with reference to the case depicted in fig. 4 we can write:

$$(12) \quad A_{ij} = \int_{b_1}^{z_{ny}} C_{ij1}^1 dz + \int_{z_{ny}}^{b_2} C_{ij2}^1 dz + \int_{b_2}^{b_3} C_{ij1}^2 dz + \int_{b_3}^{b_4} C_{ij2}^3 dz,$$

and similarly for the other matrices **B, D** and **H**.

CASE b).

In this case, the fibres being oriented at an arbitrary angle θ with respect to the global coordinate system, and the values of strains with respect to this system being known, it is necessary to calculate, by a suitable rotation matrix, the strain $\epsilon_f = \epsilon_1$ in the fibre direction:

$$(13) \quad \epsilon_f = \epsilon_{xx} \cos^2 \theta - 2\epsilon_{xy} \sin \theta \cos \theta + \epsilon_{yy} \sin^2 \theta.$$

The neutral surface position z_{nn} can be determined by replacing the strain components of (13) with those from (2), eq. (13) being held equal to zero.

$$(14) \quad z_{nn} = - \frac{\left(u_{0,x} + \frac{1}{2} w_{0,x}^2 \right) \cos^2 \theta - (u_{0,y} + v_{0,x} + w_{0,x} w_{0,y}) \sin \theta \cos \theta + \left(v_{0,y} + \frac{1}{2} w_{0,y}^2 \right) \sin^2 \theta}{\psi_{x,x} \cos^2 \theta - (\psi_{x,y} + \psi_{y,x}) \sin \theta \cos \theta + \psi_{y,y} \sin^2 \theta}$$

It is easy to note that when $\theta = 0^\circ$ we obtain z_{nz} (eq. (11a)) and when $\theta = 90^\circ$ we

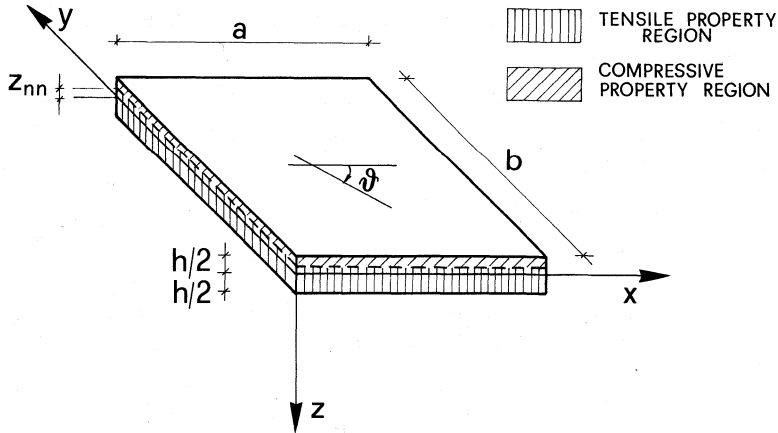


Fig. 5. - Scheme of single-layer laminate and neutral surface position.

obtain z_{ny} (eq. (11b)). Thus the calculation of A_{ij} leads to:

$$(15) \quad A_{i,j} = \int_{-b/2}^{z_{nn}} C_{ij1} dz + \int_{z_{nn}}^{b/2} C_{ij2} dz.$$

Analogously for matrices B, D and H . When a linear analysis is carried out the non-linear terms in eqs. (11a, b), and (14) must obviously be neglected.

The solution to the problem can be obtained using a stationary condition for the total energy functional [16], obtaining the following discrete equation:

$$(16) \quad \mathbf{K}\mathbf{U} = \mathbf{F}$$

where \mathbf{U} collects the nodal values of the generalized displacements u, v, w, ψ_x, ψ_y ; \mathbf{K} is the stiffness matrix of the plate and \mathbf{F} is the nodal force vector.

3. SOLUTION ALGORITHM

It should be observed that the stiffness matrix \mathbf{K} depends on the solution \mathbf{U} and its determination requires knowledge of the neutral surface position (eqs. (11a, b) or (14)).

Therefore this position is also dependent on the displacement field, *i.e.* the solution of the problem. So it is necessary to identify two iterative procedures, the first one connected to the particular constitutive model and the second to the geometrical non-linearity introduced by the von Karman model.

The global procedure is articulated in the following steps:

- 1) First it is assumed that the elastic moduli of layers are all in compression or in tension.
- 2) By a standard iterative procedure the displacement field is identified.
- 3) By the solution obtained in step 2, for each Gauss point adopted for

the numerical integration, the neutral surface position is determined by means of eqs. (11a, b) or eq. (14).

4) Now it is possible to identify which layers or which portions of the layers are in compression or in tension and then, in accordance with the philosophy of Bert's model, to define the stiffness matrix K .

5) From this stiffness matrix the new displacements of the laminate are calculated.

6) If the difference from the neutral surface position at the last step compared to the previous step is less than a pre-established tolerance the algorithm is stopped; otherwise the procedure is further iterated from step 3.

4. NUMERICAL RESULTS

a) Case studied.

In this section the formulation obtained above is used in the linear and nonlinear analysis of square and rectangular moderately thick plates.

The plates are subjected to a uniform distributed load $q = q_0$ or to a sinusoidally distributed load given by the following relation:

$$(17) \quad q = q_0 \sin(\pi x/a) \sin(\pi y/b).$$

Tables I and II contain, respectively, a list of the material's properties and boundary conditions considered here.

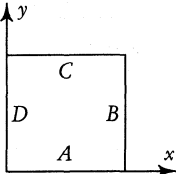
The low bimodularity ratio of the Graphite-Epoxy ($E_{1T}/E_{1C} = 1.005$), should be noted especially in comparison with the Aramid-Rubber material which presents a high bimodularity ratio ($E_{1T}/E_{1C} = 298.33$). Therefore Graphite-Epoxy is a virtually unimodular material because its behaviour when modeled as a bimodular material is not dissimilar from that obtained with only six compressive or six tensile properties.

In this work only single layer laminates were studied, while cross-ply laminates were analysed in [17] where the influence of integration of shear terms (full or reduced), the refinement of the finite element mesh and the order of the

TABLE I. - Mechanical properties of layers.

Property	Aramid-Rubber		Polyester-Rubber		Graphite-Epoxy	
	tensile	compr.	tensile	compr.	tensile	compr.
E_1 (GPa)	3.58000	0.01200	0.61700	0.03690	152.52	151.72
E_2 (GPa)	0.00909	0.01200	0.00800	0.01060	8.28	7.59
ν_{12}	0.41600	0.20500	0.47500	0.18500	0.25	0.25
G_{12} (GPa)	0.00370	0.00370	0.00262	0.00267	2.59	2.59
G_{13} (GPa)	0.00370	0.00370	0.00262	0.00267	2.59	2.59
G_{23} (GPa)	0.00290	0.00499	0.00233	0.00475	2.59	2.59

TABLE II. - Boundary conditions.



	SIDE A	SIDE B	SIDE C	SIDE D
simply supported	$u, w, \psi_x = 0$	$v, w, \psi_y = 0$	$u, w, \psi_x = 0$	$v, w, \psi_y = 0$
clamped	all edges clamped $u, v, w, \psi_x, \psi_y = 0$			

interpolation function was also studied. In the present analysis a mesh of 5×5 isoparametric nine-node quadratic elements together with reduced integration were adopted.

b) Procedure validation.

The validation of the approach to the above problem was carried out by a comparison of results of some simple cases against reliable results in the literature.

Figure 6 shows a comparison between the results of ref. [1] and those of the present work for adimensionalised centre deflection of a thin, single layer, anisotropic, unimodular clamped plate under uniform distributed load ($a/b = 2$) as the orientation angle of fibre direction θ varies.

The material considered here has the following mechanical features:

$$E_1/E_2 = 10; \quad G_{12} = G_{13} = G_{23} = 0.25 E_2, \quad \nu_{12} = 0.30.$$

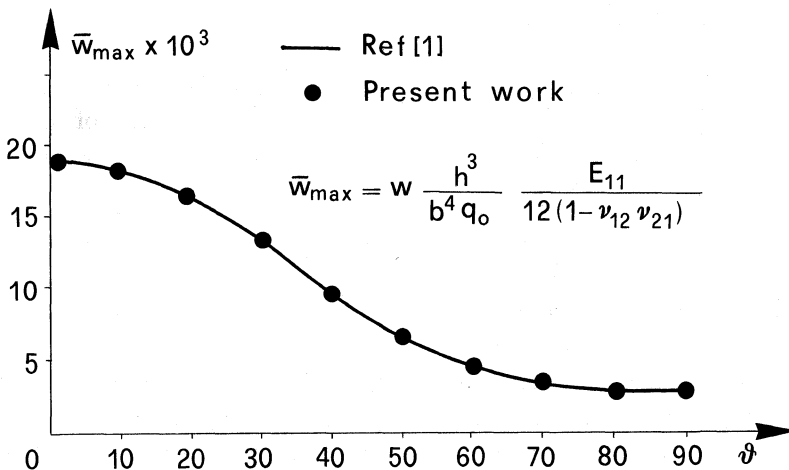


Fig. 6. - Comparison between the results of ref. [1] and those of the present work for adimensionalised centre deflection of a thin, single layer, anisotropic, unimodular clamped plate ($a/b = 2$) ($b/b = 100$) under uniform distributed load.

TABLE III. - Comparison between the dimensionless central deflection (\bar{w}) of a thin, square, single-layer, bimodular obtained in ref. [18], with that given in the present study by linear or nonlinear analysis.

\bar{q}	Aramid-Rubber		Polyester-Rubber	
	Reddy [18]	P. A.	Reddy [18]	P. A.
lineare	0.29590	0.29550	0.16830	0.16811
10	0.27200	0.27134	0.16540	0.16523
20	0.49630	0.49483	0.32330	0.32286
30	0.68210	0.68029	0.47180	0.47116
40	0.84170	0.83808	0.61060	0.60963
50	0.97980	0.97554	0.73990	0.73853

P. A.: Present Analysis.

TABLE IVa, b. - Comparison of maximum deflections and neutral surface position for bimodular single-layer, thick plates ($a/h = 10$, $\bar{w} = w(E_{2C}b^3)/(q_0b^4)10^2$, $\bar{z}_{nn} = z_{nn}/h$).

a) Polyester-Rubber

a/b	Present Analysis		Closed Form		Reddy [10]	
	\bar{w}	\bar{z}_{nn}	\bar{w}	\bar{z}_{nn}	\bar{w}	\bar{z}_{nn}
0.5	0.1955	0.30516	0.1529	0.3044	0.1971	0.3045
0.7	0.5057	0.30490	0.4283	0.3042	0.5075	0.3044
1.0	1.4315	0.30360	1.3030	0.3029	1.4300	0.3031
1.4	3.5080	0.30040	3.3480	0.2999	3.4920	0.3001
2.0	7.0470	0.29390	6.9250	0.2934	7.0030	0.2936

b) Aramid-Rubber.

a/b	Present Analysis		Closed Form		Reddy [10]	
	\bar{w}	\bar{z}_{nn}	\bar{w}	\bar{z}_{nn}	\bar{w}	\bar{z}_{nn}
0.5	0.2748	0.44570	0.2544	0.4453	0.2750	0.4454
0.7	0.7732	0.44500	0.7393	0.4447	0.7712	0.4447
1.0	2.0942	0.44220	2.0460	0.4420	2.0830	0.4420
1.4	4.3625	0.43650	4.3130	0.4363	4.3350	0.4363
2.0	7.2864	0.42560	7.2500	0.4253	7.2360	0.4254

As can be seen, the results obtained in the present analysis are in a good agreement with those given in [1].

Table III compares results obtained by considering the influence of nonlinearity in the strain-displacement eqs. (2) with those given by Reddy in [18].

This table shows the adimensionalised transverse deflections of single layer (0°), simply-supported square plates made of Aramid-Rubber and Polyester-Rubber materials under uniform distributed load ($a/h = 100$, $\bar{w} = w/b$, $\bar{q} = (q_0/E_{2C})(a/h)^4$). The values associated with the linear analysis are obtained for $\bar{q} = 10$.

TABLES Va, b. – Neutral surface position in the fibre direction and maximum deflections for simply-supported, rectangular plates of bimodular single-layer (0° , $a/b = 100$, linear analysis).

a) Polyester-Rubber

a/b	z_{nn}/b			\bar{w}		
	P. A.	C. F.	Reddy [19]	P. A.	C. F.	Reddy [19]
0.5	0.3041	0.3040	0.3041	0.0827	0.0816	0.0821
0.6	0.3042	0.3040	0.3041	0.1669	0.1655	0.1656
0.7	0.3040	0.3040	0.3039	0.2992	0.2975	0.2968
0.8	0.3037	0.3040	0.3036	0.4905	0.4888	0.4866
0.9	0.3033	0.3040	0.3031	0.7491	0.7478	0.7434
1.0	0.3027	0.3027	0.3026	1.0797	1.0790	1.0710
1.2	0.3013	0.3014	0.3012	1.9506	1.9540	1.9350
1.4	0.2996	0.2998	0.2995	3.0458	3.0560	3.0210
1.6	0.2977	0.2979	0.2976	4.2582	4.2780	4.2240
1.8	0.2955	0.2958	0.2954	5.4757	5.5050	5.4310
2.0	0.2931	0.2936	0.2931	6.6129	6.6520	6.5600

P. A.: Present Analysis, C. F.: Closed Form.

b) Aramid-Rubber.

a/b	z_{nn}/b			\bar{w}		
	P. A.	C. F.	Reddy [19]	P. A.	C. F.	Reddy [19]
0.5	0.4454	0.4457	0.4454	0.1889	0.1881	0.1875
0.6	0.4452	0.4457	0.4451	0.3670	0.3661	0.3640
0.7	0.4473	0.4457	0.4447	0.6262	0.6253	0.6211
0.8	0.4440	0.4444	0.4440	0.9685	0.9679	0.9605
0.9	0.4431	0.4444	0.4431	1.3872	1.3870	1.3760
1.0	0.4420	0.4424	0.4420	1.8690	1.8700	1.8540
1.2	0.4394	0.4398	0.4393	2.9522	2.9560	2.9280
1.4	0.4363	0.4358	0.4363	4.0828	4.0890	4.0490
1.6	0.4329	0.4334	0.4328	5.1610	5.1700	5.1200
1.8	0.4292	0.4298	0.4292	6.1346	6.1430	6.0850
2.0	0.4254	0.4260	0.4254	6.9866	6.9950	6.9310

P. A.: Present Analysis, C. F.: Closed Form.

For both materials considered the comparisons show that results are close enough to be satisfactory.

The adimensionalised central deflections and the neutral surface positions determined in the central Gauss point are given for simply-supported thick plates ($\theta = 0, 1$ layer, linear analysis) manufactured in Polyester-Rubber (table IVa) and Aramid-Rubber (table IVb) subject to a sinusoidal load as the a/b ratio varies;

TABLES Vc, d. - Adimensionalised maximum inplane displacements $\bar{u} = u_{\max}/w_{\max} \cdot 10$; $\bar{v} = v_{\max}/w_{\max} \cdot 10$.

c) Polyester-Rubber.

a/b	Present Analysis		Reddy [19]	
	\bar{u}	\bar{v}	\bar{u}	\bar{v}
0.5	0.1883	0.0856	0.1974	0.0897
0.6	0.1576	0.0719	0.1588	0.0724
0.7	0.1354	0.0607	0.1364	0.0611
0.8	0.1186	0.0517	0.1194	0.0521
0.9	0.1054	0.0445	0.1061	0.0448
1.0	0.0948	0.0388	0.0955	0.0397
1.2	0.0787	0.0303	0.0793	0.0306
1.4	0.0671	0.0248	0.0676	0.0249
1.6	0.0584	0.0208	0.0588	0.0210
1.8	0.0515	0.0181	0.0519	0.0183
2.0	0.0460	0.0160	0.0464	0.0162

d) Aramid-Rubber.

a/b	Present Analysis		Reddy [19]	
	\bar{u}	\bar{v}	\bar{u}	\bar{v}
0.5	0.2786	0.1296	0.2808	0.1306
0.6	0.2324	0.1085	0.2342	0.1093
0.7	0.1991	0.0910	0.2007	0.0917
0.8	0.1741	0.0768	0.1754	0.0774
0.9	0.1521	0.0653	0.1556	0.0658
1.0	0.1387	0.0560	0.1397	0.0565
1.2	0.1150	0.0423	0.1158	0.0427
1.4	0.0979	0.0331	0.0986	0.0334
1.6	0.0850	0.0266	0.0856	0.0269
1.8	0.0749	0.0220	0.0755	0.0222
2.0	0.0668	0.0186	0.0673	0.0188

the results obtained by a closed form [10] and Reddy's finite element analysis are also included in the table.

The values of z_{mn} are almost independent of the a/b ratio while values of \bar{w} increase with a/b . Furthermore the results compare well.

The case of thin plates subjected to sinusoidal load is studied in tables Va, b; for the same case, in tables Vc, d, besides the previous quantities, the values of adimensionalized maximum inplane displacements \bar{u} and \bar{v} are compared.

The same conclusions drawn by examining tables Va, b can be reached for the values of \bar{w} , in tables Vc, d while the opposite occurs for the values of \bar{u} and \bar{v} .

c) Investigation and discussions.

To offer evidence on the difference between the bimodular and unimodular materials' behaviour, comparisons were made among the deflections of simply-supported single-layer square plates subject to uniform distributed load considering six tensile, six compressive and twelve bimodular properties, respectively (fig. 7). In addition the deflections of thick ($a/b = 10$) and thin ($a/b = 100$) plates, both manufactured in Aramid-Rubber, are compared. The results obtained using these three different kinds of properties differ highly from each other. In fact the ratio between the deflections of bimodular and unimodular compressive plates is about 2, whereas the deflections of bimodular plates are about 4 times higher than those of unimodular tensile plates.

The case of Graphite-Epoxy material is not of interest here because, as a consequence of the low bimodularity ratio, unimodular and bimodular plates differ only slightly from each other in their behaviour.

The influence of the angle of fibre orientation on the centre deflection of a uniformly loaded, simply supported square plate is shown in fig. 8. Both

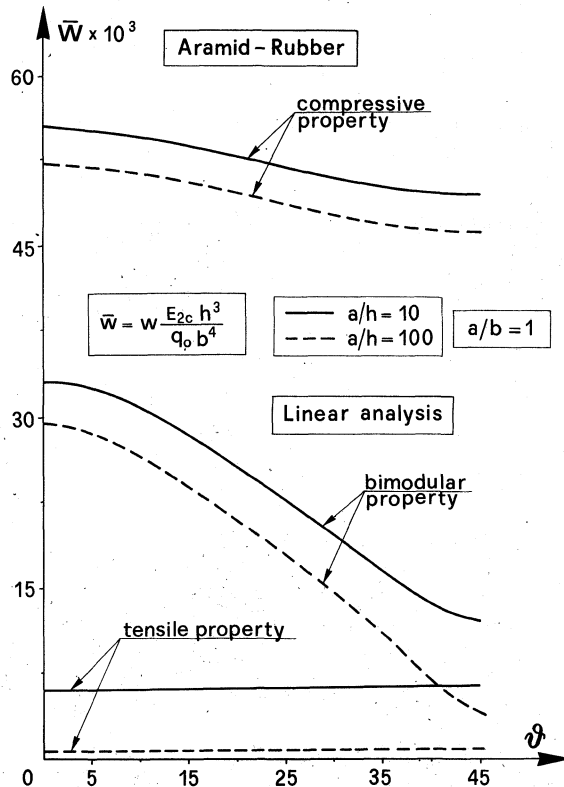


Fig. 7. - Dimensionless centre deflection of a square plate under uniform distributed load (SS1, Aramid-Rubber), using material's tensile, bimodular and compressive properties *vs.* the angle of fibre orientation.

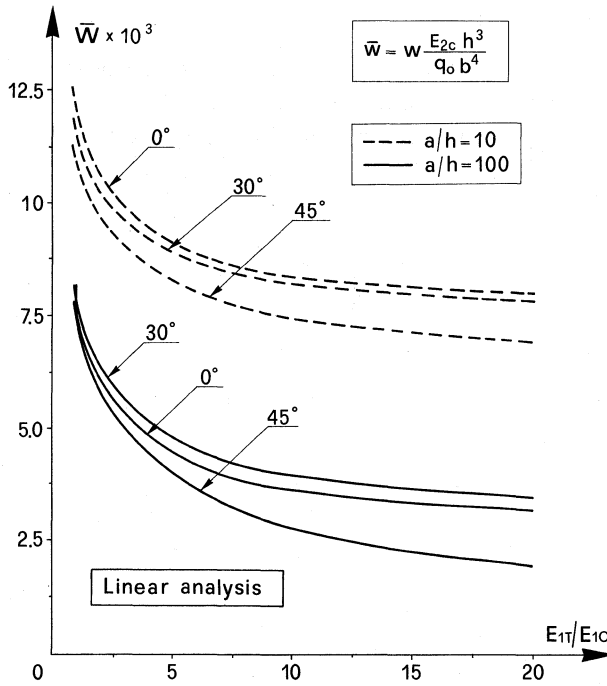


Fig. 8. - Effect of the fibre orientation on the dimensionless centre deflection of a single layer square plate under uniform distributed load.

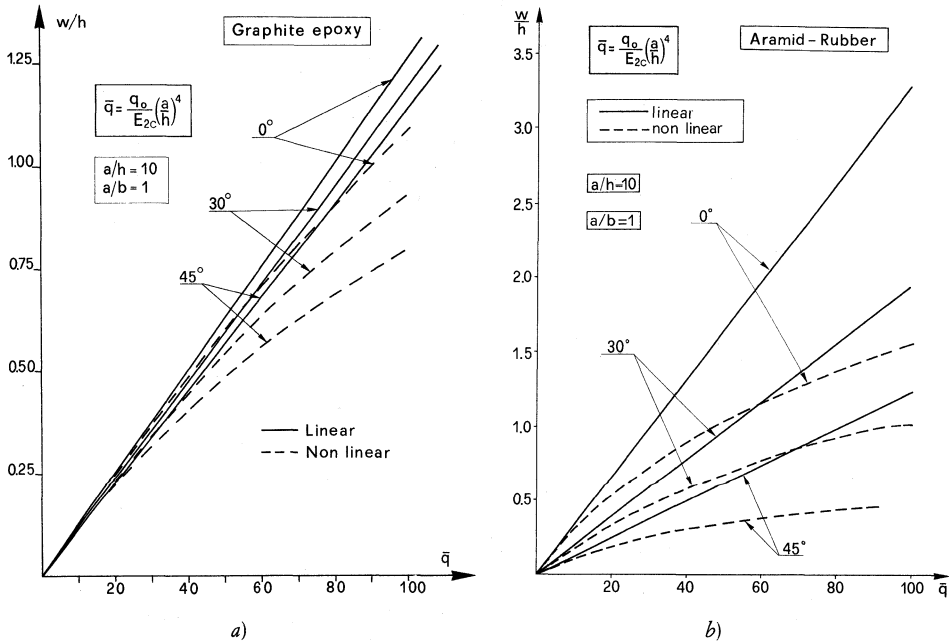


Fig. 9a, b. - Variation of central deflection with \bar{q} of single-layered square plate.

the effect of bimodularity ratio and shear deformability are taken into account.

All the properties of the material considered are those of Graphite-Epoxy except the E_{1T} modulus which varies with the bimodularity ratio E_{1T}/E_{1C} .

The centre deflection decreases as the E_{1T}/E_{1C} ratio increases; this occurs in different ways depending both on the combination of the angle of fibre orientation and for the plate thickness. In the case of a higher bimodularity ratio the variation of centre deflection with the angle θ is larger.

The effects of the angle of fibre orientation and of adimensionalised uniform load \bar{q} on the maximum deflection of single-layer, simply-supported, thick, square plates are shown in figs. 9a and 9b for Graphite-Epoxy and Aramid-Rubber materials respectively.

It should be observed that deflections are overestimated if a linear analysis is carried out. This is more pronounced if plates are manufactured in Aramid-Rubber material.

The deflections decrease as the angle of fibre direction increases in both linear and nonlinear analysis. In addition the nonlinear behaviour becomes more pronounced with the increase in θ .

Figures 10a and 10b show the adimensionalised centre deflection of single-layer, simply supported, square plates made in Graphite-Epoxy and Aramid-Rubber materials, respectively. The analysis is carried out both including von Karman's nonlinear terms and without including them in both thick and thin plates.

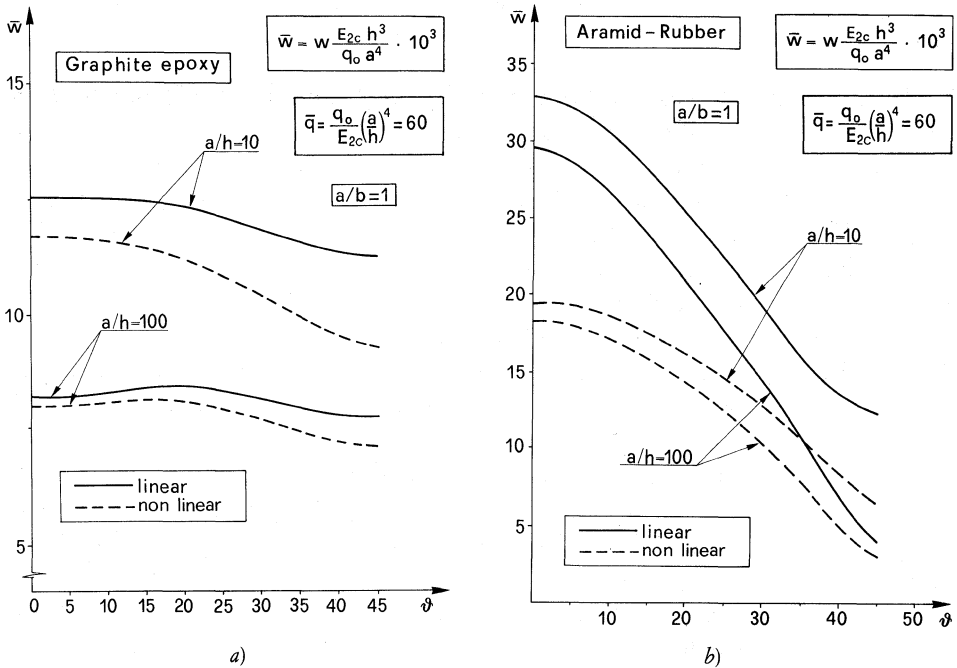


Fig. 10a, b. - Dimensionless central deflection of square, simply-supported, single-layer plates vs. the angle of fibre orientation.

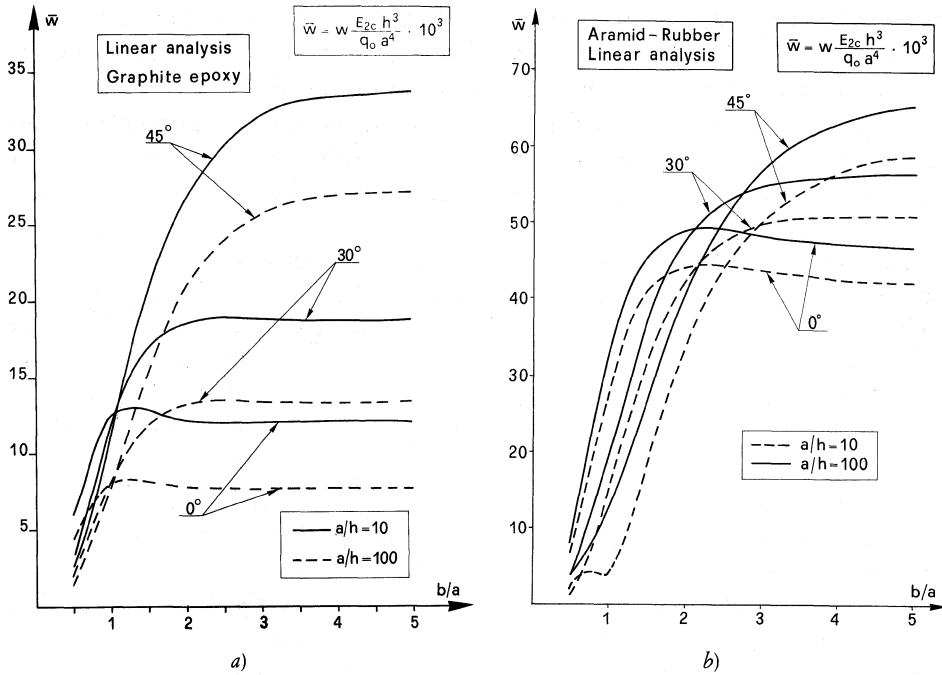


Fig. 11a, b. – Linear adimensionalised maximum deflection of simply-supported, single-layer, rectangular plates vs. the aspect ratio and angle θ .

The transverse adimensionalised load was kept high enough ($\bar{q} = 60$), to render the nonlinear behaviour sufficiently appreciable.

A clear difference between the results of linear and nonlinear analysis can be observed, especially for thick plates. The increase of the fibre direction angle produces a reduction of the plate's centre deflection.

The influence of the angle θ on the deflections is more pronounced for Aramid-Rubber which is characterized by a high bimodularity ratio.

Figures 11a and 11b show the variation of adimensionalised centre deflection vs. the b/a ratio for various angles of fibre orientation. The plates considered are single-layer, simply-supported and made in Graphite-Epoxy or Aramid-Rubber materials respectively.

In these cases the nonlinear terms in the strain-displacement relations are neglected and both Mindlin's ($a/h = 10$) and Classical Plate ($a/h = 100$) theories are considered. In addition three values of the fibre direction angle ($\theta = 0^\circ, 30^\circ, 45^\circ$) are selected.

It can be observed that when the aspect ratio increases, the adimensional centre deflection tends asymptotically to different values for each type of laminate. Passing from $\theta = 45^\circ$ to $\theta = 0^\circ$ the maximum deflection of plate decreases.

Finally the simply supported, square, cross-ply plates are analysed in figs. 11a and

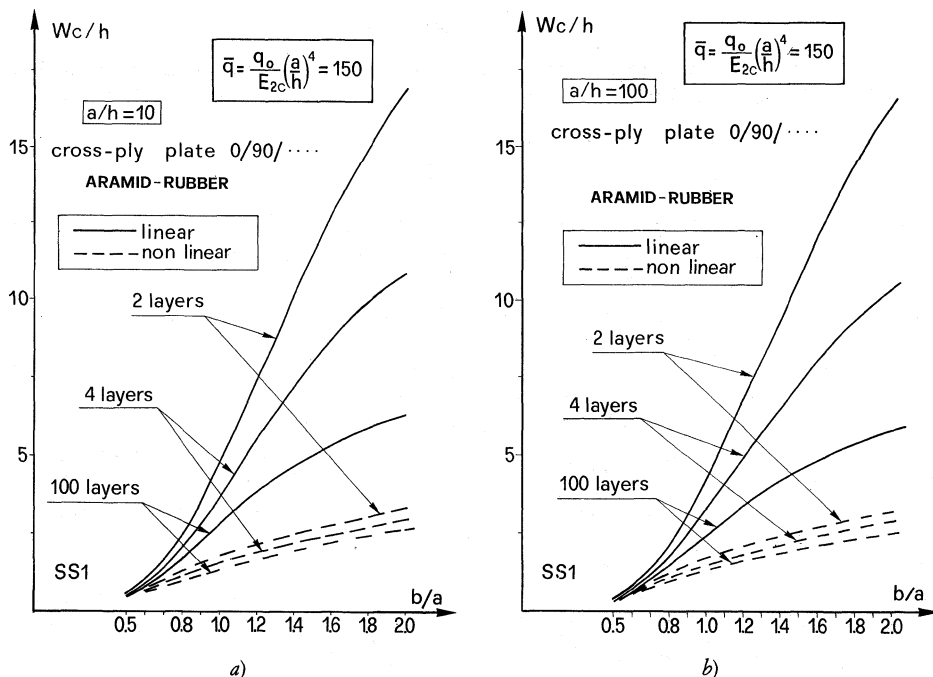


Fig. 12a, b. - Variation of central deflection with aspect ratio of rectangular cross-ply plates under uniform distributed load.

11b. The plates are both in Aramid-Rubber material, the two cases differing from each other for the a/h ratio.

The importance of including von Karman's nonlinear terms is reaffirmed because the deflections are overestimated if a linear analysis is carried out.

A cursory examination of eqs. (10) reveals that the coupling between bending and stretching, as displayed in eq. (9a), vanishes as the number of layers increases. This consideration highlights the reduction of deflections with layering.

5. CONCLUSIONS

The analysis of the results obtained in this study leads to the following conclusions:

- both the bimodularity ratio and the effect of shear deformation strongly affect the bending of composite bimodular plates;
- the transverse deflection of this kind of plate depends in particular on the fibre orientation;
- when a high bimodularity ratio occurs, the assumption of a unimodular relationship can lead to excessive errors in predicting the plate's displacements.

ACKNOWLEDGEMENTS

The authors of this work gratefully acknowledge the financial support of the Italian Ministry of Education (M.P.I. 60% quota) and the technical support of the Consorzio per le Ricerche e le Applicazioni di Informatica (C.R.A.I.).

REFERENCES

- [1] J. E. ASHTON - J. M. WHITNEY, *Theory of laminated plates*. Technomic Publishing Co. Inc., 1970.
- [2] B. SAINT VENANT, Notes to the 3rd ed. of Navier's, *Résumé des leçons de la résistance des corps solides*. Paris 1864, 175.
- [3] S. TIMOSHENKO, *Strength of materials*. In: *Advanced Theory and Problems*. 2nd ed., Van Nostrand, Princeton, New Jersey 1941, part 2, 362-369.
- [4] S. A. AMBARTSUMYAN, *The axisymmetric problem of a circular cylindrical shell made of material with different stiffnesses in tension and compression*. Izvestiya Akademiya Nauk SSSR, Mekhanika, n. 4, 1965, 77-85 (Engl. trans. National Tech. Information Center Document AD. 675312, 1967).
- [5] R. M. JONES - H. S. MORGAN, *Bending and extension of cross-ply laminates with different moduli in tension and compression*. Computers & Structures, vol. 11, 1980, 181-190.
- [6] C. W. BERT, *Models for fibrous composites with different properties in tension and in compression*. J. of Engng. Mat. Tech., Trans. of ASME 99H(4), 1977, 344-349.
- [7] S. A. AMBARTSUMYAN - A. A. KHACHATRYAN, *Basic equations in the theory of elasticity for materials with different stiffness in tension and compression*. Inzh. Zhur. MTT2, 1966, 44-53 (in Russian).
- [8] S. A. AMBARTSUMYAN, *Basic equations and relations in the theory of anisotropic bodies with different moduli in tension and compression*. Inzh. Zhur. MTT3, 1969, 51-61 (in Russian).
- [9] F. TABADDOR, *Constitutive equations for bimodulus elastic materials*. AIAA J., vol. 10(4), 1972, 516-518.
- [10] C. W. BERT - J. N. REDDY - V. SUDHAKAR REDDY - W. C. CHAO, *Bending of thick rectangular plates laminated of bimodulus composite materials*. AIAA J., vol. 19(10), 1981, 1342-1349.
- [11] R. D. MINDLIN, *Influence of rotatory inertia and shear on flexural motions of isotropic elastic plates*. J. of Appl. Mech., 1951, 31-38.
- [12] T. VON KARMAN, *Festigkeitsprobleme in Maschinenbau*. Encycl. Math. Wiss., vol. 4, 1910, 348-351.
- [13] T. VON KARMAN - E. E. SECHLER - L. H. DONNELL, *The strength of thin plates in compression*. Trans. ASME, vol. 54, 1932, 53-57.
- [14] F. GORDANINEJAD, *Nonlinear bending of anisotropic bimodular composite plates*. Computers & Structures, vol. 33, 1989, 615-620.
- [15] F. GORDANINEJAD, *A finite element model for the analysis of thick, anisotropic, bimodular, fibrous-composite plates*. Computers & Structures, vol. 31, 1989, 907-912.
- [16] G. PORCO - G. SPADEA - R. ZINNO, *A geometrically nonlinear analysis of laminated composite plates using a shear deformation theory*. Atti Acc. Lincei Rend. fis., s. 8, vol. 83, 1989, 159-176.
- [17] D. BRUNO - G. PORCO - R. ZINNO, *Finite element analysis of nonlinear laminated composite plates*. Proceedings of International Meeting UPSA IV (Capri, June 14-16, 1989).
- [18] J. N. REDDY - W. C. CHAO, *Nonlinear bending of bimodular-material plates*. Int. J. Solids Structures, vol. 19, n. 3, 1983, 229-237.
- [19] J. N. REDDY - W. C. CHAO, *Finite-element analysis of laminated bimodulus composite material plates*. Computers & Structures, vol. 12, 1980, 245-251.

G. Porco e G. Spadea: Dipartimento di Strutture - Facoltà di Ingegneria
Università degli Studi della Calabria
87030 ARCAVACATA DI RENDE CS

R. Zinno: C.N.R. - C.R.A.I.
87030 S. STEFANO DI RENDE CS